Talanta 273 (2024) 125826

Contents lists available at ScienceDirect

Talanta

journal homepage: www.elsevier.com/locate/talanta

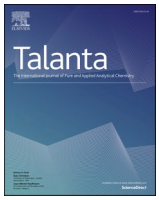

Tear metabolomics for the diagnosis of primary open-angle glaucoma

Marina Botello-Marabotto [a,b,c], M. Carmen Martínez-Bisbal [a,b,c,d,*], M. Dolores Pinazo-Durán [e,f,g,1], Ramón Martínez-Máñez [a,b,c,h,i,1]

[a] Instituto Interuniversitario de Investigación de Reconocimiento Molecular y Desarrollo Tecnológico (IDM), Universitat Politècnica de València – Universitat de València, Valencia, Spain
[b] Unidad Mixta de Investigación en Nanomedicina y Sensores, Instituto de Investigación Sanitaria La Fe (IISLAFE) - Universitat Politècnica de València, Valencia, Spain
[c] CIBER de Bioingeniería, Biomateriales y Nanomedicina, Instituto de Salud Carlos III, Spain
[d] Departamento de Química Física, Universitat de València, Valencia, Spain
[e] Ophthalmic Research Unit "Santiago Grisolia"/FISABIO, Valencia, Spain
[f] Cellular and Molecular Ophthalmobiology Research Group at the University of Valencia, Valencia, Spain
[g] Spanish Net of Inflammatory Research (REI-RICORS: RD21/0002/0032) Institute of Health Carlos III, Madrid, Spain
[h] Departamento de Química, Universitat Politècnica de València, Valencia, Spain
[i] Unidad Mixta UPV-CIPF de Investigación en Mecanismos de Enfermedades y Nanomedicina, València, Universitat Politècnica de València, Centro de Investigación Príncipe Felipe, Valencia, Spain

ARTICLE INFO

Handling Editor: Prof A Campiglia

Keywords:
Primary open angle glaucoma
Metabolomics
^{1}H NMR spectroscopy
Biomarkers
Diagnosis

ABSTRACT

Primary Open-Angle Glaucoma (POAG) is the most prevalent glaucoma type, and the leading cause of irreversible visual impairment and blindness worldwide. Identification of early POAG biomarkers is of enormous value, as there is not an effective treatment for the glaucomatous optic nerve degeneration (OND). In this pilot study, a metabolomic analysis, by using proton (^{1}H) nuclear magnetic resonance (NMR) spectroscopy was conducted in tears, in order to determine the changes of specific metabolites in the initial glaucoma eyes and to discover potential diagnostic biomarkers. A classification model, based on the metabolomic fingerprint in tears was generated as a non-invasive tool to support the preclinical and clinical POAG diagnosis. ^{1}H NMR spectra were acquired from 30 tear samples corresponding to the POAG group (n = 11) and the control group (n = 19). Data were analysed by multivariate statistics (partial least squares-discriminant analysis: PLS-DA) to determine a model capable of differentiating between groups. The whole data set was split into calibration (65%)/validation (35%), to test the performance and the ability for glaucoma discrimination. The calculated PLS-DA model showed an area under the curve (AUC) of 1, as well as a sensitivity of 100% and a specificity of 83.3% to distinguish POAG group versus control group tear data. This model included 11 metabolites, potential biomarkers of the disease. When comparing the study groups, a decrease in the tear concentration of phenylalanine, phenylacetate, leucine, n-acetylated compounds, formic acid, and uridine, was found in the POAG group. Moreover, an increase in the tear concentration of taurine, glycine, urea, glucose, and unsaturated fatty acids was observed in the POAG group. These results highlight the potential of tear metabolomics by ^{1}H NMR spectroscopy as a non-invasive approach to support early POAG diagnosis and in order to prevent visual loss.

1. Introduction

Glaucoma is the second leading cause of blindness worldwide after cataracts, with the differential characteristic of becoming irreversible due to the progressive damage to the retinal ganglion cells (RGCs) and optic nerve fibres (ONFs). This injury leads to optic atrophy, peripheral vision decline, and loss of vision-related quality-of-life, also constituting an important matter of global socio-economic burden [1,2]. Glaucoma affects more than 70 million people worldwide and it is estimated that 111.8 million by 2040 will develop the disease [3,4].

The most common glaucoma type is primary open angle glaucoma (POAG), which is characterized by mechanical insult due to the elevated intraocular pressure (IOP), morphological alteration of the optic nerve head, and functional landmarks, as the progressive visual field loss,

* Corresponding author. Departamento de Química Física, Universitat de València, C/ Doctor Moliner, 50, 46100 Burjassot, Valencia, Spain.
E-mail address: carmen.martinez-bisbal@uv.es (M.C. Martínez-Bisbal).
[1] These two authors (M.D.P.-D.; R.M.-M.) are sharing last place as the study coordinators.

https://doi.org/10.1016/j.talanta.2024.125826
Received 3 November 2023; Received in revised form 14 February 2024; Accepted 21 February 2024
Available online 25 February 2024

Table 1
Inclusion and exclusion criteria for the study participants.

POAG group	control group
INCLUSION	
Diagnosis of POAG	Healthy non-glaucomatous individuals
Aged **>40 and < 80 years**	Aged <40 and <80 years
Initial glaucoma stage	–
Precise data at the clinical records	Precise data at the clinical records
Psychic and physical status that permits the participation in the study	Psychic and physical status that permits the participation in the study
EXCLUSION	
Other Glaucoma type	–
Aged **<40 and > 80 years**	Aged <40 and >80 years
Other glaucoma stage	–
Other eye diseases or recent ophthalmic laser/surgery.	Other eye diseases or recent ophthalmic laser/surgery
Other systemic diseases/treatments/ surgery	Other systemic diseases/treatments/ surgery
Missing data or incomplete clinical history	Missing data or incomplete clinical history
No able to participate	No able to participate

constituting a neurodegenerative process, globally known as the glaucomatous OND [2,5]. Unfortunately, POAG is asymptomatic in the early stages. The only therapeutic action is the prompt initiation of elevated IOP treatment, and no neuroprotective treatments are currently available in clinical practice [5]. However, the medical-laser-surgical hypotensive glaucoma therapy does not prevent disease progression or visual impairment [6]. In spite of the advances in epidemiological and experimental studies, more research is needed on the molecular mechanisms responsible for the glaucoma development and progression [7]. Reliable biomarkers for early glaucoma diagnosis are yet to be discovered [8].

A singular set of metabolites, named metabolome, is the result of the combination of genetic and environmental factors, among others, that is found in a biological sample. Genomics, transcriptomics, proteomics and metabolomics constitute the biological omics cascade [9,10]. The metabolome gives information more directly related to the phenotype than any other omics science [9,10]. Mainly, two sophisticated techniques, mass spectrometry (MS) [11,12], and nuclear magnetic resonance (NMR) spectroscopy [12,13], lead the determination of metabolomic profiles. NMR spectroscopy is a robust and reproducible method that allows to determine the metabolic composition of biofluids (blood derivatives, cerebrospinal, urine, tears, saliva, sweat, synovial, etc.) usually through very simple preparation procedures and using small amount of sample, being these two features the most relevant in the clinical context [14,15]. Both techniques need computationally intensive statistical tools to refine interpretation [11–15].

When POAG diagnosis and prognosis is approached, a key issue to address is the selection of a suitable biologic sample to provide information on the pathology [16–18]. Most studies agree in the use of blood for biomedical glaucoma research, but also aqueous humor, vitreous body, and tear samples have been used, as recently reviewed by Tezel [19]. Our research group has conducted extensive research on the pathophysiology of ocular diseases, mainly ocular surface disorders, glaucoma, and diabetic retinopathy, by using tear samples [20–24]. Another key point in glaucoma research is to select the most suitable participants for the study, according to an accurate diagnosis, and to make an appropriate classification of the disease stage [2,5,7,8].

Some metabolites and metabolic pathways associated to pathological processes have been reported to be altered in glaucoma, mainly regarding carbohydrates [25], amino acids [25,26], and fatty acids [27], along with inflammation and neurodegeneration pathways. However, it has not yet been possible to identify a panel of reliable biomarkers that can be obtained non-invasively for translation as a diagnostic and prognostic tool to the clinical practice.

Aimed for this context, in this work we intended to develop a non-invasive method to support the diagnosis and prognosis of POAG patients at the initial stage of the disease, based on the tear metabolomic fingerprinting obtained by ^{1}H NMR spectroscopy. The secondary objective is to search for potential biomarkers of the disease, to help increase knowledge about the molecular processes underlying the clinically asymptomatic initial steps of the glaucomatous OND.

2. Materials and methods

2.1. Focused topic and study characteristics

There is no cure for glaucoma. There is growing interest in identifying and validating clinical, imaging, biochemical, and molecular-genetic biomarkers that may help early detection of POAG. To progress in knowledge on the clinical and molecular basis of POAG, a collaborative multicenter analytical case-control pilot study was planned for 50 male and female participants aged 40–80. This work was conducted in accordance with the tenets of the Declaration of Helsinki (Edimburgh 2000), reviewed and approved by the Institutional Boards (code: 131/18; code P14_23_01_19). All clinical requirements to maintain the data privacy from the study participants were specifically met. All volunteers were informed and signed the consent to participate.

2.2. Eligibility requirements for the study participants

Ophthalmic specialists caring for glaucoma patients carried out a pre-selection by personal interview, according to the inclusion/exclusion criteria listed in Table 1. Socio-demographics, personal and family characteristics, lifestyle, and treatments were recorded in a Microsoft Excel spreadsheet, as DEMO. A systematized ocular examination was done in the potential participants that got an appointment for the eye clinic. Best-corrected visual acuity (BCVA) was obtained from each eye calculating the logarithm of the minimum angle of resolution (LogMAR). The IOP was measured by Goldman applanation tonometry (Haag-Streit AT 900; Haag-Streit Köniz, Switzerland). Morphological determination (indirect gonioscopy) through a slit-lamp (IMAGEnet, Topcon, Barcelona, Spain) with the Goldmann 3-mirror lens was carried out to identify an open anterior chamber angle; ocular fundus exploration with a 78D lens was performed through a slit-lamp; examination by optical coherence tomography (OCT) (Cirrus spectral-domain OCT, Carl Zeiss Meditec, Inc., Madrid, Spain) of the anterior and posterior eye segments, and functional probes by means of the visual field (VF) performance, using the 24-2 Swedish interactive threshold algorithm (Humphrey field analyzer, Carl Zeiss Meditec, Inc., Madrid, Spain), were also carried out. For the evaluation of participants, standard definitions of IOP, central corneal thickness (CCT), cup-to-disc (C/D) ratio, retinal nerve fiber layer (RNFL) thickness, RGCs density and VF median deviation (MD) were applied. In this context, normal IOP was considered as <21 mmHg, and any IOP above this threshold was defined as ocular hypertension (OHT). The CCT was determined by OCT and the normal values were estimated at 533 μm.

Participants were classified as POAG group if they met one of these criteria: 1) patients previously diagnosed and confirmed in the clinical history as initial glaucomatous OND, under hypotensive eye drop therapy (Latanoprost, Timolol, and/or Brinzolamide); 2) naïve POAG cases with corrected IOP/CCT higher than 21 mmHg, with an initial glaucomatous OND including specific optic nerve head alterations such as neuroretinal rim thinning, peripapillary nerve fiber loss, asymmetry of cupping between the patient eyes, and parapapillary atrophy, etc. Glaucoma damage was staged into the adequate category for better managing the disease. In this concern, automated VF is the hallmark for testing the visual function in glaucoma patients. We have used static automated perimetry (SAP) for the GPAA diagnosis by the Humphrey Swedish Interactive Thresholding Algorithm (SITA) 24-2 Fast, with fixation monitoring and gaze-tracking (Humphrey visual field analyzer; Carl Zeiss Meditec, Madrid, Spain). In this study population, glaucomatous defects have been detected using the above techniques, with the reliability indices of the European Glaucoma Society (EGS), mean

Fig. 1. Reflex tear collection from the inferior lacrimal meniscus by capillarity.

Table 2
Ophthalmic characteristics of the study participants.

Parameters	POAG group	control group	p value
BCVA RE	0.2	0.0	<0.05
BCVA LE	0.2	0.1	<0.05
IOP RE (mm Hg)	20 ± 2	14 ± 1	<0.001
IOP LE (mm Hg)	19 ± 2	15 ± 1	<0.001
CCT RE (μm)	527 ± 13	575 ± 12	<0.01
CCT LE (μm)	532 ± 12	568 ± 14	<0.01
Average C/D ratio RE	0.6 ± 0.2	0.1 ± 0.01	<0.001
Average C/D ratio LE	0.5 ± 0.3	0.1 ± 0.01	<0.001
Average RNFL thickness RE (μm)	70 ± 10	94 ± 11	<0.05
Average RNFL thickness LE (μm)	72 ± 8	89 ± 10	<0.05
RCCs density RE	65 ± 8	94 ± 12	<0.001
RGCs density LE	68 ± 9	90 ± 12	<0.001
VF MD RE	−3.2 ± 1.6	-1dB ± 1	<0.001
VF MD LE	−2.5 ± 1.2	-1dB ± 1	<0.001

BCVA: best corrected visual acuity; logMAR: logarithm of the minimum angle of resolution; VF MD: visual field mean deviation; RE: right eye, LE: left eye; IOP: intraocular pressure; CCT: central corneal thickness; C/D: cup-to-disc; RNFL: retinal nerve fiber layer.

deviation (MD) and pattern standard deviation (PSD). The MD corresponds to the mean elevation or depression in the VF, as compared to the reference normal VF. According to the MD values, it was classified as mild, moderate, or severe VF damage (>6.00 dB, −6.01 a 12.00 dB, and <12.01 dB, respectively) [28]. The PSD corresponds to the irregularity measurements, in each of 6 regions of the VF, by adding the absolute value of the difference between the threshold value for each point, and the average VF sensitivity at each point. Therefore, according to the Hodapp et al. [28], approach, minimum criteria for considering the initial glaucoma stage is: 1) a glaucoma hemifield test outside normal limits (in at least two VF); 2) a cluster of three or more non-edge points in a location typical for glaucoma, all of which are depressed on the pattern deviation plot at a $p < 5\%$ level, and one of which is depressed at a $p < 1\%$ level (on two consecutive VF); 3) a corrected pattern standard deviation that occurs in less than 5% of normal VF (on two consecutive VF performances). Within the VF indexes, it has to be contemplated that the MD is the average elevation/depression of visual sensitivity in the overall VF, compared with that of the normal age-corrected reference VF. Therefore, the classification of VF defects for early glaucoma includes: 1) VF mean deviation less than −6 dB; 2) Less than 25% of the points are depressed below the 5% level and less than 10 points are depressed below the 1% level on the pattern deviation plot; and 3) All point in the central 5° must have a sensitivity of at least 15 dB.

Participants were classified as control group when the IOP was lower than 21 mm Hg with normal visual fields, optic disc, and RNFL in absence of other ocular or systemic disease (as in the inclusion/exclusion criteria).

All data were recorded into a Microsoft Excel spreadsheet, as OPHTHAL, which was reviewed by the glaucoma specialist. At baseline, a total of 50 individuals were selected by a nonrandom consecutive sampling procedure, to better confirm the health and ocular condition of the suitable participants and were distributed into two groups: patients with POAG diagnosis (n = 23) and individuals without glaucoma, as a control group (n = 27). Final sample size of our pilot study participants was 30 (11 POAG patients and 19 control individuals). Changes in the potential number of participants were due to the volunteer decision, clinical issues, and/or sampling contingences. Recruitment characteristics and operative procedures are depicted in Figure S1.

2.3. Sample collection

Reflex tears were collected through capillarity by using a microhematocrit tube from each eye of the study participants, by a gentle rubbing of the inferior meniscus and external canthus of each eye, without instilling anaesthetics as described elsewhere [20–24]. A tear volume ranging from 6 to 25 μL was collected from each participant. Each sample was transferred into micro Eppendorf tubes, appropriately labelled and stored at −80 °C until processing. A total of 30 samples were collected from POAG patients (n = 11), and the control group (n = 19), as previously described [20–24]. Fig. 1 shows the sampling technique for collecting reflex tears from the study participants.

2.4. Sample preparation for ^{1}H NMR spectroscopy study

Before sample preparation, tears were thawed. To prepare each sample, 20 μL of tear fluid were introduced in NMR tubes with a diameter of 1,7 mm. The remaining volume was completed up to 60 μl with phosphate buffer (which additionally contained deuterated water and the internal standard sodium 2,2-dimethyl-2-silapentane-5-sulphonate (DSS) 1 mM), following previously published procedures [29]. In three cases the volume of tear available was less than 20 μl (6, 15 and 16 μL respectively). In those cases, extra quantity of phosphate buffer was added to complete the volume of 60 μL. Following the same procedure, three of the pharmacological active principles of the topical glaucoma therapy were considered for better classifying our participants, as those administered in monotherapeutic regimen or in association [Lumigan® (Bimatoprost), Azopt® (Brinzolamide) and Azarga® (Timolol/-Brinzolamide)] and were prepared for NMR spectroscopy acquisition, to rule out that any of the signals included in the analyses were directly produced by the presence of the drugs.

2.5. NMR spectra acquisition and processing

The samples underwent NMR spectroscopy study (Príncipe Felipe Research Center Foundation (CIPF) NMR facility). NMR spectra were acquired using a 600 MHz spectrometer (Bruker AVII-600, Bruker Biospin, Germany) equipped with a 5 mm TCI cryoprobe (^{1}H, $^{15}N^{13}C$), a temperature unit BCU05 and a refrigerated SampleJet. The temperature of the probe was set at 300 K (27 °C). ^{1}H NMR monodimensional spectra were acquired for each sample with noesy pulse sequence and presaturation of the water signal during the relaxation time and mixing time. 200 scans were programmed with a spectral width of 30 ppm. Following the same procedures ^{1}H NMR noesy spectra were as well acquired from the topical drugs used for ocular hypertension treatment. The chemical shift of the signals from the drugs spectra were taken into consideration in later analyses. Once acquired, the spectra were transformed and preprocessed. For the pre-processing of the spectra an exponential line-broadening function of 0.5 Hz was applied followed by Fourier transformation with TopSpin 3.6.2. Phasing, baseline correction and chemical shift calibration to DSS resonance at 0.0 ppm was done with the program MestReNova version 6.0.2 (Mestrelab Research SL, Santiago de

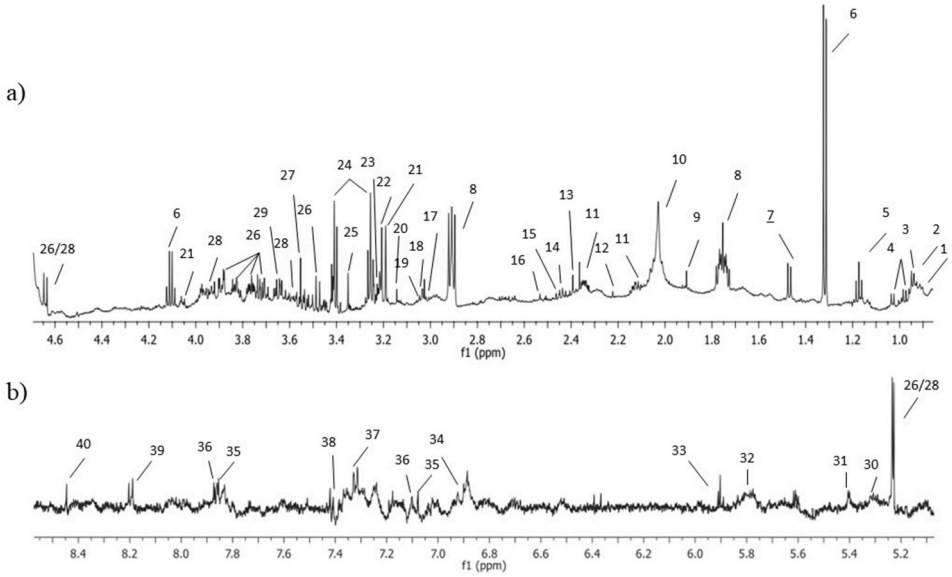

Fig. 2. ^{1}H NMR spectrum of one tear sample. The residual water signal (4.7–5.1 ppm) is not shown a) Aliphatic region of the spectrum (0.8–4.6 ppm) b) Aromatic region of the spectrum (5.2–8.5 ppm). The intensity of peaks in the aromatic region (5.0–8.7 ppm) has been scaled (5x) respect to the aliphatic region for a more appropiated display. 1. Fatty Acids (–CH_3), 2. Isoleucine, 3. Leucine, 4. Valine, 5. Ethanol, 6. Lactate, 7. Alanine, 8. DSS, 9. Acetate, 10. N-acetyled compounds, 11. Glutamate, 12. Acetone, 13. Pyruvate, 14. Pyroglutamic Acid, 15. Glutamine, 16. Citrate, 17. Creatine, 18. Creatinine, 19. Lysine, 20. Dimethyl Sulfone, 21. Choline, 22. Carnitine, 23. Arginine, 24. Taurine, 25. Methanol, 26. Glucose, 27. Glycine, 28. Glucose 6-phosphate, 29. Glycerol, 30. Unsaturated Fatty Acids, UFA (-CH═CH-), 31. Sucrose, 32. Urea, 33. Uridine, 34. Tyrosine, 35. Histidine, 36. Histamine, 37. Phenylacetate, 38. Phenylalanine, 39. Hypoxanthine, 40. Formic acid.

Compostela, Spain). Areas from the different peaks in the 1D ^{1}H spectra were integrated. The integrated areas were used to determine the differences in metabolite concentration between tears from CG and POAGG. The peaks were assigned according to their chemical shift and the information in different databases, such as the human metabolome database (HMDB) [30] and the biological magnetic resonance data bank (BMRB) [31].

2.6. Statistical analysis

2.6.1. General statistical proceedings

Statistics for the clinical data were performed by the *IBM SPSS 28.0* program (IBM SPSS Statistics for Windows, Version 28.0. Armonk, NY: IBM Corp). The Shapiro-Wilk test (subgroups) and the Kolmogorov-Smirnov test (main groups) were used to verify the normal distribution of the quantitative variables, whereas the qualitative variables were described by absolute and relative frequencies. Quantitative variables were described using the mean and standard deviation (normal distribution) or median and interquartile range (non-normal distribution). Differences between quantitative variables were analysed using the Student's *t*-test for independent samples and ANOVA (normal variable) or the Mann-Whitney and Kruskal Wallis *U* test (non-normal variable). Differences between groups were considered statistically significant when the p-value was less than or equal to 0.05.

To determine the metabolomic differences between tears from the POAG and the control groups, statistical analysis was performed. The integration data from each peak was normalized to the sum of all signals and auto-scaled. These data were fed into the software *PLS_Toolbox Solo 8.9* (Eigenvector Research, Inc., Manson, WA, USA) to perform multivariate statistical analysis. A Principal Component Analysis (PCA) was employed to determine the presence of outsiders, to remove them from further analysis.

Partial Least Squares-Discriminant Analysis (PLS-DA) was used to generate a predictive model, able to classify the samples based on the relative concentration of metabolites in each group. The data were split into calibration (2/3 of the samples were used for the generation of the model) and validation (1/3 of the samples was used to prove the discriminative capacity of the generated model in an independent data set) subsets. The variables included in the model were iteratively selected based on its Variable Importance in Projection (VIP) value until reaching the optimization of the model. Cross Validation (venetian blinds) was used to select the optimal number of latent variables for the model. In order to determine the goodness of the model to discriminate between different sets of samples, the area under the ROC curve value (AUC), the sensitivity and the specificity were calculated. After validation, the robustness and over-fitting of the model were tested through permutation test (100 iterations, Rand-t-test, Wilcoxon and Sign test). p-value <0.05 was considered significant.

Univariate analysis of the metabolites participating in the model was performed by using *Metaboanalyst* [32]. The mean of normalized intensity for each metabolite was calculated for the two groups, POAG and control groups. The *t*-test was used to determine significant differences between metabolites in POAG and control tear samples after testing the normality of the variables. False Discovery Rates (FDR) adjusted p-values were as well obtained and considered for statistical significance.

2.6.2. Analysis of altered metabolic pathways

Metaboanalyst [32] was used to explore the potential metabolic pathways involved in the pathological processes. HMDB ID of each metabolite was used to include them in the pathway analysis. The global test enrichment analysis selected for the topological analysis was relative-betweenness centrality. The pathways with p-value <0.05 and impact factor >0 were selected as representative pathways.

3. Results

3.1. Patient characteristics

Final number of participants in this pilot study was 30 (11 POAG patients and 19 control individuals), as depicted in figure S1. The breakdown of participants was 20 (40%), that failed to complete the study for a variety of reasons, including loss of interest and volunteer drop out, experimenter error, clinical findings, and alterations in

Table 3
Chemical shift, multiplicity and J coupling of the signals from metabolites identified in the tear samples.

Number	Metabolite	Chemical Shift (ppm) and J coupling (Hz)[a]
1	Fatty Acids (–CH_3),	0.8–0.9
2	Isoleucine	0. 93 (t, J = 7.0), 1 (d, J = 6.5), 1.31 (m)
3	Leucine	0.97 (d), 0.98 (d), 1.72 (m)
4	Valine	1.01 (d, J = 7.2), 1.06 (d, J = 7.2)
5	Ethanol	1.16 (t, J = 7.08), 3.67 (q, J = 7.07)
6	Lactate	1.35 (d, J = 7.0), 4.14 (c, J = 7.0)
7	Alanine	1.47(d, J = 7.2), 3,77 (q, J = 7.2)
8	DSS	0.00 (s), 1.75 (m), 2.92 (t)
9	Acetate	1.91 (s)
10	N-acetyled compounds	2.0–2.1
11	Glutamate	2.11 (td, J = 6.8, 6.2), 2.15 (dt, J = 15.4, 6.8), 3.75 (t, J = 6.2)
12	Acetone	2.22 (s)
13	Pyruvate	2.36 (s)
14	Pyroglutamic acid	2.39 (m), 2.50 (m), 4.17 (dd, J = 9.02, 5.83)
15	Glutamine	2.42 (dt, J = 14.4, 6.8), 3.76 (t, J = 6.2)
16	Citrate	2.52 (d, J = 15.4), 2.66 (d, J = 15.4)
17	Creatine	3.02 (s), 3.92 (s)
18	Creatinine	3.03 (s), 4.05 (s)
19	Lysine	1.46 (m), 1.71 (m), 1.89 (m), 3.02 (t), 3.74 (t, J = 6.09)
20	Dimethyl sulfone	3.14 (s)
21	Choline	3.19 (s), 3.51 (dd, J = 5.81, 4.16), 4.05 (ddd)
22	Carnitine	2.13 (s), 2.48 (dd, J = ND), 2.61 (dd, J = ND), 3.18 (s), 3.61 (d, J = ND), 3.82 (dd, J = ND), 5.57 (q)
23	Arginine	1.68 (m), 1.90 (m), 3.23 (t, J = 6.93), 3.76 (t, J = 6.11)
24	Taurine	3.25 (t, J = 6.57), 3.42 (t, J = 6.62)
25	Methanol	3.34 (s)
26	Glucose	3.74 (d, J = 5.4), 3.81 (dt, J = 8.4,5.4), 5.22 (d, J = 1.6)
27	Glycine	3.55 (s)
28	Glucose 6-phosphate	3.27 (dd, J = 9.21, 7.99), 3.71 (t, J = 9.54), 4.64 (d, J = 7.99), 5.22 (d, J = 3.75)
29	Glycerol	3.58 (dd), 3.67 (dd, J = 11.7, 4.3) y 3.90 (m)
30	UFA	5.25–5.35
31	Sucrose	3.46 (t, J = 9.30), 3.55 (dd, J = 3.98, 3.89), t (3.75),
32	Urea	5.78 (s)
33	Uridine	3.801 (dd, J = 12.77, 4.4), 4.21 (m), 4.22 (dd),
34	Tyrosine	6.91 (m), 7.21 (m)
35	Histidine	3.16 (dd, J = 15.55, 7.7), 3.23 (dd, J = 16.10, 4.9), 3.98 (dd, J = 7.73, 4.98), 7.09 (d, 0.58), 7.90 (d, J = 1.13)
36	Histamine	3.03 (m), 3.29 (t, J = 7.11), 7.14 (s), 7.99 (s)
37	Phenylacetate	3.53 (s), 7.29 (m), 7.36 (m)
38	Phenylalanine	7.35 (m), 7.39 (m), 7.44 (m)
39	Hypoxanthine	8.17 (s), 8.20 (s)
40	Formic acid	8.44 (s)

[a] Multiplicity is indicated as s (singlet), d (doublet), t (triplet), q (quadruplet), m (multiplet).

sampling, transportation, or laboratory processing of the biological samples.

Mean age was 69 ± 8 years (71 ± 9 years in the POAG group and 68 ± 7 years in the control group). Gender distribution was 64% women/36% men in the POAG group and 55% women/45% men in the control group. The mean age and gender distribution were not significantly different between POAG and control groups. All participants were Caucasian.

3.2. Systemic and ophthalmologic clinical characteristics

Comorbidities were recognized non-IOP risk factors for the POAG course, and the following were taken into consideration in the study participants: hypertension blood pressure, cardiovascular disease, diabetes mellitus, myopia, and/or obesity (increased body mass index). The participants with the above disorders were excluded from the study, according to the criteria established in Table 1 (figure S1).

The POAG patients had IOP elevation, verified through the augmented optic disc excavation, optic nerve damage, and altered VF. The participants in POAG group were under glaucoma treatment (hypotensive eye drops as monotherapy: 52% Bimatoprost (Lumigan ®), and 8% Brinzolamide (Azopt ®), as well as fixed combination: 40% Timolol/Brinzolamide (Azarga ®)). The CG was constituted by those healthy individuals without any of the above glaucoma milestones.

Ophthalmological examination showed that mean BCVA LogMAR was 0.00 for the RE (right eye) and 0.10 for the LE (left eye) in the CG, versus 0.20 (RE) and 0.20 (LE) in the POAG group. Moreover, the mean IOP, and the mean CCT were significantly lower in the control group respect to the POAG group ($p < 0.001$; $p < 0.001$). The most important OCT and VF parameters were the mean cup-to-disc ratio, RNFL thickness, and RGCs density, as well as the VF MD and PSD. Overall, the SAP data analyses showed a significant decrease in MD values ($p < 0.001$), and a significant increase in the PSD values ($p < 0.001$) in the POAG patients respect to the controls. In fact, the POAG patients displayed mild VF damage. No moderate or severe VF damage was detected in our glaucomatous population. All the above parameters were significantly different between both study groups. The ophthalmological parameters of the study for both groups and the p-values are shown in Table 2.

3.3. ^{1}H NMR spectroscopy study

Finally, 30 tear samples corresponding to both eyes of the study participants (POAGG n = 11; CG n = 19) were analysed by ^{1}H NMR metabolomics.

3.3.1. ^{1}H NMR profile of tears obtained from the study participants

^{1}H NMR noesy spectra were acquired for all tear samples and drugs (Lumigan ®, Azopt ® and Azarga ®). The spectra showed an acceptable signal to noise ratio, despite the low concentration of the metabolites in the samples, enough to enable the assignment and the relative quantification of the signals. The main signals in tears were assigned and are shown in Fig. 2. The spectrum is shown divided into two parts, aliphatic (Fig. 2a) and aromatic (Fig. 2b), to enable a better observation of the signals. A total of 40 metabolites were assigned according to their chemical shifts, multiplicity and J coupling (Table 3). The spectra of the drugs were also obtained and are shown in figure S2, to assess that the signals in the discriminant models between POAG and control groups are not due to the treatments.

3.3.2. Multivariate data analysis of the tear metabolomic profiles

In order to identify the presence of outliers or significant clustering of POAG and control tear samples, an unsupervised PCA analysis was performed with the relative concentrations of the different metabolites. Some clustering related to the presence or absence of the disease could already be appreciated in the undirected classification analysis, based on the scores of the samples in the principal components one and two (Fig. 3a). Two samples, one POAG and one control, were located outside the 95% confidence level at the PCA diagram and were removed from further studies.

The remaining samples (from 18 controls and 10 POAG patients) were randomly divided into two groups (calibration and validation), to perform a PLS-DA analysis. The model was generated with the calibration subset, through the iterative selection of the most representative variants (VIP >1). When applied to the validation subset, the ROC curve of the model showed excellent classification capacity with an AUC value of 1 (Fig. 3b). This model predicted with high sensibility (100%) and specificity (83.3%) if the tear samples were from control or POAG (Fig. 3c). Wilcoxon permutation test provided a $p < 0.05$, which confirmed the robustness of the model to discriminate between both groups. From the 40 identified metabolites, the multivariate model included 11 of them to discriminate POAG group from control group: phenylalanine, phenylacetate, leucine, taurine, glycine, urea, glucose, n-

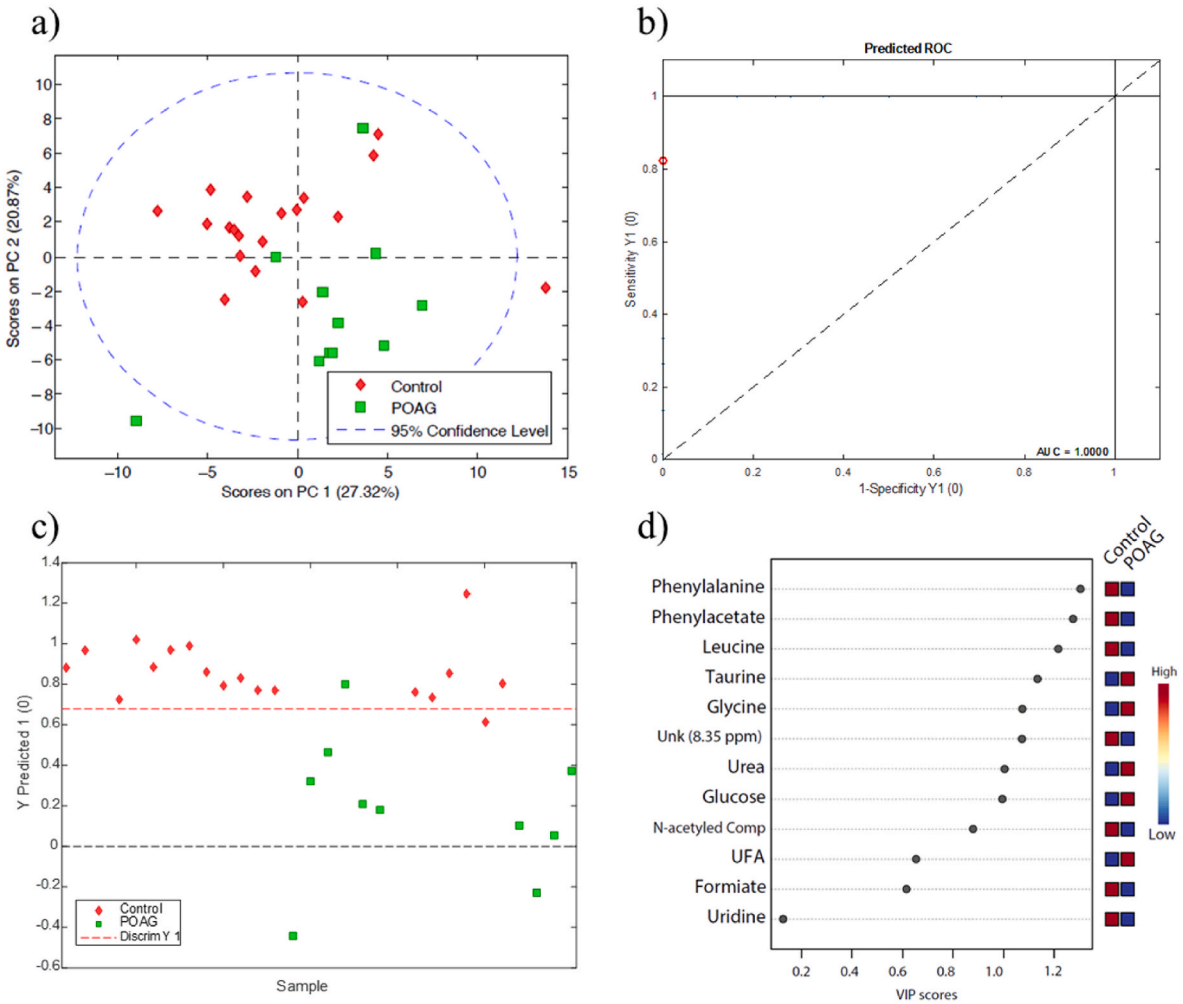

Fig. 3. Multivariate statistical analysis. Data from control group are presented in red diamonds and data from POAG group are presented in green squares in a) and c). a) Principal component analysis (PCA) for the whole set of samples to determine outliers b) ROC curve of the model c) Partial least squares-discriminant analysis. (PLS-DA) score plot. The classification of calibration (left) and validation (right) samples is shown d) Variables participating in the prediction model. The VIP values of the metabolites and its relative changes in control and POAG group is displayed. (red = increaed in POAG group vs. control group, blue = decreased in POAG group vs. control group).

acetyled compounds, UFA, formic acid and uridine, as well as an unassigned species at 8.35 ppm (unk 8.35 ppm). For this final model, the most relevant metabolites with a VIP >1 were phenylalanine, phenylacetate, leucine, taurine, glycine, urea and glucose (Fig. 3d).

3.3.3. *Mean comparison of metabolites included in the discriminative model*

Afterwards, the relative concentration of the metabolites with discriminative capacity, as shown in the multivariate classification model was studied (Fig. 4, Table 4). All metabolites, with the exception of formic acid and uridine, showed significant difference with a FDR <0.05. The analysis showed a decrease in the relative concentration of phenylalanine, phenylacetate, leucine, n-acetyled compounds, formic acid, uridine and unk (8.35 ppm) in POAG tear samples compared to the tears from control group. On the other hand, an increase in the concentration of taurine, glycine, urea, glucose and UFA in tears of POAG group was observed.

Furthermore, the relative concentration of the discriminant metabolites is displayed in a clustering heatmap, where the metabolites are clustered together according to their relative increase/decrease in control and POAG samples, and samples are clustered according to their metabolites' profile (Fig. 5). The cluster analysis showed that all the samples are clustered with their group except two of them. This clustering is in agreement with the classification observed in the PLS-DA model (Fig. 3c).

3.3.4. *Metabolic Pathways analysis*

Quantitative pathway topological analysis of the metabolites included in the discriminative model, revealed significant alterations in phenylalanine metabolism, taurine and hypo-taurine metabolism, glyoxylate and dicarboxylate metabolism, glycine, serine and threonine metabolism, glutathione metabolism, phenylalanine, tyrosine and tryptophan biosynthesis, primary bile acid biosynthesis and glycolysis/gluconeogenesis (Fig. 6, Table 5).

4. Discussion

In this pilot study, we investigated the metabolites present in tear samples from POAG patients and controls by ^{1}H NMR spectroscopy to generate, through multivariate statistics, a predictive model able to identify patients at initial glaucoma stage, at risk of OND and vision loss. We found that the generated model showed excellent discriminant ability with an AUC of 1, and 100% of sensibility and 83.3% of specificity in the classification of POAG group and control group. From the statistical model generated, a list of potential biomarkers of the disease, and associated metabolic pathways were obtained. Moreover, changes in the concentration of biomarkers involved in the discriminant model

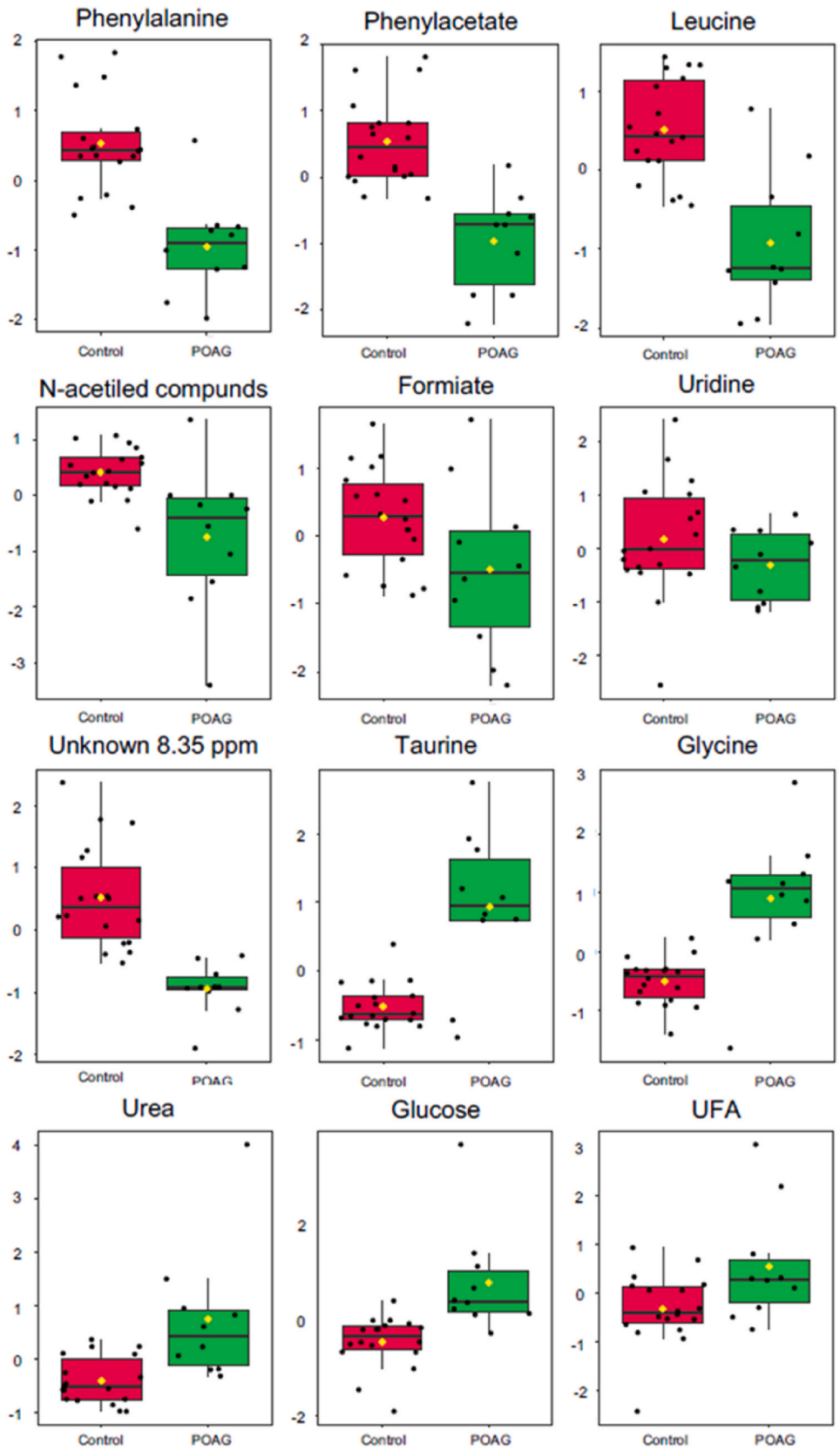

Fig. 4. Comparison of the mean concentration of the metabolites participating in the discriminative model. Box plots representing the mean concentration of normalized metabolites in control and POAG tears samples are shown. The yellow diamonds represent the mean and the horizontal line the median of each group for a determined feature. The normalized concentrations of each sample are shown as black dots.

Table 4
Relative mean concentrations of discriminative metabolites between control and POAG groups, and statistical significance of normalized data.

	[Metab][a]		p-value	FDR[b]
	control group	POAG group		
Phenylacetate	50.6	19.6	9.12E-06	7.26E-05
Phenylalanine	51.9	20.9	1.21E-05	7.26E-05
Unknown (8.35 ppm)	0.8	0.2	2.05E-05	7.43E-05
Taurine	8.5	10.9	2.48E-05	7.43E-05
Leucine	48	25.4	3.68E-05	8.83E-05
Glycine	13	13.5	5.82E-05	1.16E-04
Glucose	0.3	0.9	5.52E-04	9.46E-04
Urea	26.6	41.4	1.69E-03	2.29E-03
N-acetyled compounds	114.2	67.6	1.72E-03	2.29E-03
UFA (-CH═CH-)	0.3	0.5	0.024	0.028
Formic acid	0.3	0.1	0.049	0.054
Uridine	14.8	7.9	0.22	0.22

[a] Relative mean concentration in control group and POAG group are shown x10^3.
[b] FDR: False discovery Rate.

were confirmed by the significant differences shown in the univariate analysis. A descent in the relative concentration of phenylalanine, phenylacetate, leucine, n-acetyled compounds, formic acid, uridine and unk (8.35 ppm), and an increment in the concentration of taurine, glycine, urea, glucose and UFA in tears was found in the POAG group as compared to the control group.

The discovery of molecular biomarkers in tears could reveal essential information regarding POAG pathophysiology, as well as help to manage medical-laser-surgical hypotensive therapy [2–4,7,8,21,23,28]. In this context, early diagnosis and treatment are pivotal to avoid glaucoma progression, optic atrophy, and blindness [28,33]. It is essential to consider that: i) a significant number of patients present at first medical appointment with elevated IOP and moderate-to-severe VF loss, due to the silent period of undetected OHT, and ii) some glaucoma patients suffer higher rates of progression than others. Therefore, some findings have been reached in the present work that could be transferred to ophthalmic practice, which are discussed below.

First, tear samples were used for the metabolomic study in glaucoma, in agreement with Agnifili et al. [34], and Wu et al. [35], and in contrast with other authors usually using aqueous humor or plasma samples for this purpose [25,26,36–38]. As widely known, the tear film is located on the outermost part of the ocular surface, in direct contact with the environment. Under normal conditions, tear volumes range from 4 to 12 μL per eye [39]. The tear film is a complex and interesting biological fluid that contains water and a wide variety of electrolytes, lipids, proteins, glycoproteins and small molecules from different sources [39–41]. After a period of controversy, it has been established that metabolites associated with glaucoma present in the tear film mainly come from the aqueous humor, through the uveoscleral outflow pathway, after precise scleral percolation [39–41]. Trying to counteract the small tear volumes that can be collected for analytical issues, a technique for obtaining reflex tears by gentle rubbing of the inferior lacrimal meniscus and palpebral lateral canthus, has been used here, to relatively easy obtaining 20–30 μL of tears from both eyes by capillarity, as described elsewhere [20–24].

Next, we analysed the metabolites in tears from POAG patients at initial stage of disease, according to Hodapp et al. [28], but at risk of glaucoma OND and blindness. Epidemiological and experimental studies have established that the early detection of OHT, and the prompt IOP reduction significantly diminish the risk of glaucoma progression [2–5,33]. This stage is very important, because the elevated IOP leads to progressive damage and death of the RGCs and optic fibre loss, glaucoma hallmarks that manifests themselves in the structural/functional ophthalmological examination of these patients. However, there are no specific and complete standard references for accurately establishing the early glaucoma diagnosis [2–5,28,33]. Bearing this in mind, the POAG group was accurately selected for the main purpose of this study, that was to characterize the metabolomic fingerprint in tears of POAG patients at initial stage of disease in order to identify potential biomarkers for better eye and vision care.

Furthermore, ^{1}H NMR spectroscopy was used to generate, through multivariate statistics, a predictive model able to identify POAG patients at initial glaucoma stage. Biomedical and biotechnological advances in metabolomics have provided information on a considerable number of metabolites to better understand the metabolic changes that occur in glaucoma. Previous reports on the identification of metabolomic biomarkers of glaucoma by MS have been performed using blood and aqueous humor samples [26,41–46]. However, other researchers used ^{1}H NMR spectroscopy, as in this study, to perform glaucoma metabolomics, either using blood or aqueous humor samples, with optimum results [33,47].

Data are quite different among the studies. In spite of describing the biological sample and the analytical platform, the statistical processing as well as the changes of the statistically significant metabolites identified in a differential profile, important variations arise that make it difficult to identify potential biomarkers of glaucoma. Leruez et al. [37] described amino acids, carbohydrates and polyamine families, among others, altered in POAG samples and associated to mitochondrial dysfunction, senescence and polyamines deficiency. However, they did not explore the diagnosis potential of the metabolites identified. Myer

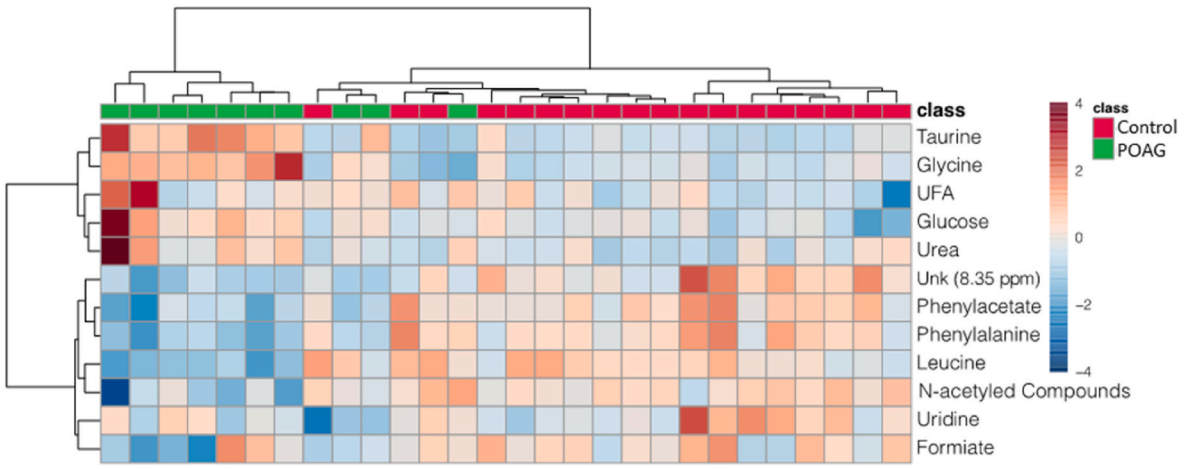

Fig. 5. Heat map with the concentration of the metabolites participating in the discriminative model. Metabolites are clustered according to its relative increase (red)/decrease (blue).

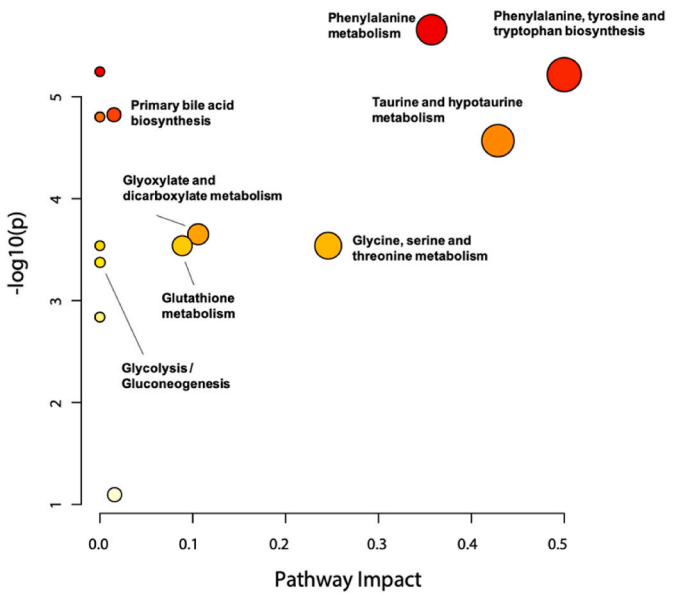

Fig. 6. Significant metabolic pathways altered in POAG group compared to control group. Each circle represents an identified metabolic pathway. The size of the circle is proportional to the pathway impact value (PIV) and the colour is proportional to the statistical significance [-$\log_{10}$(p)] from highest (red) to lowest (white).

Table 5
Significant metabolic pathways and pathway impact values obtained from integrating enrichment analysis and pathway topology analysis.

Metabolic Pathway	Total Cmp[a]	Hits	p - value	FDR[b]	Impact
Phenylalanine metabolism	10	2	2.20E-06	3.04E-05	0.36
Phenylalanine, tyrosine and tryptophan biosynthesis	4	1	6.07E-06	3.04E-05	0.50
Primary bile acid biosynthesis	46	2	1.50E-05	3.94E-05	0.02
Taurine and hypotaurine metabolism	8	1	2.70E-05	5.78E-05	0.43
Glyoxylate and dicarboxylate metabolism	32	2	2.24E-04	3.95E-04	0.11
Glycine, serine and threonine metabolism	33	1	2.89E-04	3.95E-04	0.25
Glutathione metabolism	28	1	2.89E-04	3.95E-04	0.09
Glycolysis/Gluconeogenesis	26	1	4.23E-04	5.28E-04	0.00021

[a] Cmp: Compounds.
[b] FDR: False Discovery Rate.

et al. [36] pointed out disturbances in the concentration of several amino acids, such as arginine, cysteine, threonine and lysine, and carbohydrates in the aqueous humor of POAG patients compared to the CG, and generated cross-validated PLS-DA models with Q2 values of 0.15. Better significance for the classification was reached by Buisset et al. [37] who obtained a model able to classify samples from the POAG patients with an AUC of 0.89.- Moreover they pointed out to taurine and spermine deficiency in aqueous humor from POAG patients.

From the statistical model generated in the present work, a list of potential biomarkers of the disease, and associated metabolic pathways were obtained. An increase in the concentration of taurine, glycine, urea, glucose and UFA and a decrease in the concentration of phenylalanine, phenylacetate, leucine, n-acetyled compounds, formic acid, uridine and unk (8.35 ppm) was observed in tears from the POAG group as compared to the control group. Moreover, according to these results, the phenylalanine metabolism and phenylaniline, tyrosine and tryptophan biosynthesis pathways were altered in POAG tears with a significant decrease in the concentration of phenylalanine and phenylacetate. Phenylalanine had already been pointed as a potential biomarker of glaucoma in previous metabolomic studies, both in aqueous humor, and in tears [41,43], in which the authors observed a decrease in the concentration of phenylalanine in POAG patients in a similar manner to us. Previous studies have as well reported mutations in the synthesis pathway of phenylalanine related to POAG development [48]. The significant change in the glycine, leucine and serine pathway, with the decrease in the relative concentration of leucine [41] and the relative increase in the concentration of the amino acid glycine [41,43] were also previously reported in aqueous humor. Furthermore, the increase in glucose levels observed in tears from the POAG patients presented herein is consistent with the pathological processes associated to glaucoma, as it has been reported that patients with POAG present glucose hypometabolism [49]. Also the increase in serum glucose levels has been associated with elevated IOP [50], which is strongly associated with glaucoma. An increase in the relative concentration of taurine has been detected in the present work, while previous reports noticed a decreased concentration in aqueous humor [37] and tears [41]. Taurine has a neuroprotective effect against inflammation, oxidative stress, and osmotic stress. Nevertheless, taurine could as well be produced as a counteracting mechanism against oxidative stress. In fact, in agreement with our current results, taurine was observed to increase in other previous studies conducted with aqueous humor of POAG patients [47], and in a canine [51] and rat [52] glaucoma models.

Tear metabolomic signature of POAG patients by ^{1}H NMR spectroscopy, has been described in this work. The small quantity of sample available (in the order of 20 μL) and the inherent low concentration of metabolites in tear samples have been overcome by using a high field NMR spectrometer equipped with a cryoprobe. This experimental setting has provided a non-invasive way to provide samples and data related to ocular disease. A statistical model for the diagnosis of POAG has been developed using samples obtained in a non-invasive way. Moreover, a group of potential biomarkers of the disease has been obtained from the statistic model. Future improving of this study includes the consideration of a higher number of samples, and the use of samples from patients naïve to treatment. Despite the analysis of the topical drugs assessed that the classification of the samples and the potential biomarkers obtained in this study were not directly derived from the treatment, the changes observed in the POAG samples spectra might be produced by the metabolism of the therapy. Furthermore, unlike blood derivatives that circulate through the general bloodstream, tears that come into contact with the eye can serve as a valuable source of biomarkers for glaucoma and can be collected in a non-invasive manner in contrast to aqueous humor. Previous works have studied the metabolic profile of POAG in tears by different methods of MS [35,41]. However, unlike NMR [12–14,32], MS platform requires more elaborated preparation procedures for the analysis of each sample [11,12,15,32].

Overall, data presented herein provided a model with a very good performance for disease prediction, from samples that have been obtained both by a non-invasive collecting technique (tears) and through an analytical method that requires a simplest sample preparation procedure (NMR) in contrast with previous reports that use aqueous humor and MS. Moreover, these data were also used to generate and validate the model with a spare group of samples. In conclusion, a model able to classify with great values of specificity and sensitivity POAG and control groups in an independent set of samples has been here obtained. Phenylalanine, phenylacetate, leucine, formic acid, n-acetyl compounds, uridine, taurine, glycine, urea, glucose, UFA and an unknown metabolite (8.35 ppm) could be considered potential biomarkers of patients at the initial glaucoma stage, that can be obtained in a non-invasive, relatively affordable way to improve eye and vision care. In this sense, it seems to us that pathological changes occurring in the eyes can be reflected in the whole ocular constituents, including the ocular

surface, either via local and systemic circulation, and/or via simple diffusion through the cornea and sclera. Nonetheless, by analysing tear film samples for target metabolites, we can design a promising window for optimizing POAG diagnosis and preventing blindness. This research could be a starting point for developing a non-invasive diagnostic system for POAG. In fact, we manage for the first time a new approach on the identification of POAG-related metabolites in tears, to improve the personalized diagnosis of the disease, that allows to early identify patients at highest risk of POAG or POAG progression. Future directions necessarily include the increment of the number of samples to confirm the results here shown.

CRediT authorship contribution statement

Marina Botello-Marabotto: Data curation, Formal analysis, Investigation, Visualization, Writing – original draft. **M. Carmen Martínez-Bisbal:** Investigation, Methodology, Project administration, Writing – review & editing. **M. Dolores Pinazo-Durán:** Conceptualization, Funding acquisition, Resources, Supervision, Writing – review & editing. **Ramón Martínez-Máñez:** Conceptualization, Funding acquisition, Resources, Supervision, Writing – review & editing.

Declaration of competing interest

The authors declare the following financial interests/personal relationships which may be considered as potential competing interests:

M.Carmen Martínez-Bisbal has patent #ES290219 A1 issued to Universitat de Valencia, Universitat Politècnica de Valencia, FISABIO. Ramón Martínez-Máñez has patent #ES290219 A1 issued to Universitat de Valencia, Universitat Politècnica de Valencia, FISABIO. Marina Botello-Marabotto has patent #ES290219 A1 issued to Universitat de Valencia, Universitat Politècnica de Valencia, FISABIO. Maria Dolores Pinazo-Durán has patent #ES290219 A1 issued to Universitat de Valencia, Universitat Politècnica de Valencia, FISABIO. If there are other authors, they declare that they have no known competing financial interests or personal relationships that could have appeared to influence the work reported in this paper.

Data availability

Data will be made available on request.

Acknowledgments

This research was supported, in part by: 1) project PID2021-126304OB-C41 funded by MCIN/AEI/10.13039/501100011033/and by European Regional Development Fund - A way of doing Europe, 2) Generalitat Valenciana (CIPROM/2021/007), 3) Universitat Politècnica de València and FISABIO through the POLISABIO Research Program (PI2022_02), 4) General Sub-Directorate of Networks and Cooperative Research Centers of the Carlos III Health Institute, Spanish Ministry of Economy, Industry and Competitiveness, and by the European Program FEDER, to the Spanish Research Network of Prevention, Early Detection, Treatment and Rehabilitation of Ophthalmic Pathology (OFTARED: RD16/0008/002), 5) Spanish Ministry of Science and Innovation program Cooperative Research Networks Oriented to Health Results (RICORS), to the Spanish Research Net of Inflammation and immunopathology of organs and systems REI RICORS, of the Carlos III Health Institute (RD21/0002/0032) and the European Program FEDER Next Generation EU. 6) CIBER -Consorcio Centro de Investigación Biomédica en Red- (CB07/01/2012), Instituto de Salud Carlos III, Ministerio de Ciencia e Innovación. U26 NMR: Biomedical Applications II platform from Nanbiosis (Research Infrastructures & Services of CIBER-BBN) is also gratefully acknowledged. Finally, M. Botello Marabotto acknowledges Spanish Government for her PhD grant (FPU20/05279).

Appendix A. Supplementary data

Supplementary data to this article can be found online at https://doi.org/10.1016/j.talanta.2024.125826.

References

[1] R.R.A. Bourne, J.D. Steinmetz, M. Saylan, A.M. Mersha, A.H. Weldemariam, T. G. Wondmeneh, C.T. Sreeramareddy, M. Pinheiro, M. Yaseri, C. Yu, M. S. Zastrozhin, A. Zastrozhina, Z.J. Zhang, S.R.M. Zimsen, N. Yonemoto, G. W. Tsegaye, G.T. Vu, A. Vongpradith, A.M.N. Renzaho, M.B. Sorrie, A.A. Shaheen, W.S. Shiferaw, V.Y. Skryabin, A.A. Skryabina, G.K. Saya, V. Rahimi-Movaghar, M. Shigematsu, M.A. Sahraian, H. Naderifar, S. Sabour, P. Rathi, B. Sathian, T. R. Miller, A. Rezapour, L. Rawal, H.Q. Pham, U. Parekh, V. Podder, O. E. Onwujekwe, M. Pasovic, N. Otstavnov, H. Negash, S. Pawar, M.D. Naimzada, A. Al Montasir, F.A. Ogbo, M.O. Owolabi, K. Pakshir, Y. Mohammad, M.A. Moni, V. Nunez-Samudio, G.F. Mulaw, M. Naveed, S. Maleki, I.M. Michalek, S. Misra, S. N. Swamy, J.A. Mohammed, S. Flaxman, E.C. Park, P.S. Briant, G.G. Meles, K. Hayat, I. Landires, G.R. Kim, X. Liu, K.E. LeGrand, H.R. Taylor, S.M. Kunjathur, T.A.M. Khoja, B.K. Bicer, R. Khalilov, A. Hashi, G.A. Kayode, V.L.A. Carneiro, T. Kavetskyy, S. Kosen, V. Kulkarni, R. Holla, R. Kalhor, S. Jayaram, S.M.S. Islam, S.A. Gilani, S. Eskandarieh, M.D. Molla, R. Itumalla, F. Farzadfar, N.G. Congdon, H. R. Elhabashy, R. Elayedath, R.A.S. Couto, N. Dervenis, E.A. Cromwell, S.M. A. Dahlawi, S. Resnikoff, R.J. Casson, A. Abdoli, J.Y.J. Choi, F.L.C. Dos Santos, W. A. Abrha, S.B. Nagaraja, A. Abualhasan, T.G. Adal, B.B. Aregawi, M. Beheshti, E. Abu-Gharbieh, A. Afshin, H. Ahmadieh, S.A. Alemzadeh, A. Arrigo, D.D. Atnafu, C. Ashbaugh, E. Ashrafi, W. Alemayehu, A.S. Alfaar, V. Alipour, E.W. Anbesu, S. Androudi, J. Arabloo, A. Arditi, E. Bagli, A.A. Baig, T.W. Bärnighausen, M. B. Parodi, A.S. Bhagavathula, N. Bhardwaj, P. Bhardwaj, K. Bhattacharyya, A. Bijani, M. Bikbov, M. Bottone, T. Braithwaite, A.M. Bron, Z.A. Butt, C.Y. Cheng, D.T. Chu, M.V. Cicinelli, J.M. Coelho, X. Dai, R. Dana, L. Dandona, R. Dandona, M. A. Del Monte, J.P. Deva, D. Diaz, S. Djalalinia, L.E. Dreer, J.R. Ehrlich, L.B. Ellwein, M.H. Emamian, A.G. Fernandes, F. Fischer, D.S. Friedman, J.M. Furtado, S. Gaidhane, G. Gazzard, B. Gebremichael, R. George, A. Ghashghaee, M. Golechha, S. Hamidi, B.R. Hammond, M.E.R. Hartnett, R.K. Hartono, S.I. Hay, G. Heidari, H. C. Ho, M. Househ, S.E. Ibitoye, I.M. Ilic, J.J. Huang, M.D. Ilic, A.D. Ingram, S.S. N. Irvani, R.P. Jha, R. Kahloun, H. Kandel, A.S. Kasa, J.H. Kempen, M. Khairallah, E.A. Khan, R.C. Khanna, M.N. Khatib, J.E. Kim, Y.J. Kim, A. Kisa, S. Kisa, A. Koyanagi, O.P. Kurmi, V.C. Lansingh, J.L. Leasher, N. Leveziel, H. Limburg, N. Manafi, K. Mansouri, C. McAlinden, S.F. Mohammadi, A.H. Mokdad, A.R. Morse, M. Naderi, K.S. Naidoo, V. Nangia, H.L.T. Nguyen, K. Ogundimu, A.T. Olagunju, S. Panda-Jonas, K. Pesudovs, T. Peto, M.H. Ur Rahman, P.Y. Ramulu, D.L. Rawaf, S. Rawaf, N. Reinig, A.L. Robin, L. Rossetti, S. Safi, A. Sahebkar, A.M. Samy, J. B. Serle, M.A. Shaikh, T.T. Shen, K. Shibuya, J. Il Shin, J.C. Silva, A. Silvester, J. A. Singh, D. Singhal, R.S. Sitorus, E. Skiadaresi, A. Soheili, R.A.R.C. Sousa, D. Stambolian, E.G. Tadesse, N. Tahhan, M.I. Tareque, F. Topouzis, B.X. Tran, M. K. Tsilimbaris, R. Varma, G. Virgili, N. Wang, Y.X. Wang, S.K. West, T.Y. Wong, J. B. Jonas, T. Vos, Causes of blindness and vision impairment in 2020 and trends over 30 years, and prevalence of avoidable blindness in relation to VISION 2020: the Right to Sight: an analysis for the Global Burden of Disease Study, Lancet Global Health 9 (2021) e144–e160, https://doi.org/10.1016/S2214-109X(20)30489-7.

[2] A. Greco, M.I. Rizzo, A. De Virgilio, A. Gallo, M. Fusconi, M. de Vincentiis, Emerging concepts in glaucoma and review of the literature, Am. J. Med. 129 (2016) 1000.e7–1000.e13, https://doi.org/10.1016/j.amjmed.2016.03.038.

[3] Y.C. Tham, X. Li, T.Y. Wong, H.A. Quigley, T. Aung, C.Y. Cheng, Global prevalence of glaucoma and projections of glaucoma burden through 2040: a systematic review and meta-analysis, Ophthalmology 121 (2014) 2081–2090, https://doi.org/10.1016/j.ophtha.2014.05.013.

[4] V.V. Kapetanakis, M.P.Y. Chan, P.J. Foster, D.G. Cook, C.G. Owen, A.R. Rudnicka, Global variations and time trends in the prevalence of primary open angle glaucoma (POAG): a systematic review and meta-analysis, Br. J. Ophthalmol. 100 (2016) 86–93, https://doi.org/10.1136/BJOPHTHALMOL-2015-307223.

[5] A.C. Gauthier, J. Liu, Neurodegeneration and neuroprotection in glaucoma, Yale J. Biol. Med. 89 (2016) 73–79.

[6] R. Conlon, H. Saheb, I.I.K. Ahmed, Glaucoma treatment trends: a review, Can. J. Ophthalmol. 52 (2017) 114–124, https://doi.org/10.1016/j.jcjo.2016.07.013.

[7] G. Beykin, J.L. Goldberg, Molecular biomarkers for glaucoma, Curr. Ophthalmol. Rep. 7 (2019) 171–176, https://doi.org/10.1007/s40135-019-00213-0.

[8] S. Bua, C.T. Supuran, Diagnostic markers for glaucoma: a patent and literature review (2013-2019), Expert Opin. Ther. Pat. 29 (2019) 829–839, https://doi.org/10.1080/13543776.2019.1667336.

[9] C. Johnson, J. Ivanisevic, G. Siuzdak, Metabolomics: beyond biomarkers and towards mechanisms, Nat. Rev. Mol. Cell Biol. 17 (2016) 451–459.

[10] O.A.H. Jones, Illuminating the dark metabolome to advance the molecular characterisation of biological systems, Metabolomics 14 (2018) 1–11, https://doi.org/10.1007/s11306-018-1396-y.

[11] S.J. Kim, H.E. Song, H.Y. Lee, H.J. Yoo, Mass spectrometry-based metabolomics in translational research, Adv. Exp. Med. Biol. 1310 (2021) 509–531, https://doi.org/10.1007/978-981-33-6064-8_19.

[12] A.H.M. Emwas, The strengths and weaknesses of NMR spectroscopy and mass spectrometry with particular focus on metabolomics research, Methods Mol. Biol. 1277 (2015) 161–193, https://doi.org/10.1007/978-1-4939-2377-9_13/FIGURES/14.

[13] D. Bizzarri, M.J.T. Reinders, M. Beekman, P.E. Slagboom, E.B. van den Akker, BBMRI-NL, 1H-NMR metabolomics-based surrogates to impute common clinical risk factors and endpoints, EBioMedicine 75 (2022) 103764, https://doi.org/10.1016/j.ebiom.2021.103764.

[14] G.A. Nagana Gowda, D. Raftery, NMR-based metabolomics, Adv. Exp. Med. Biol. 1280 (2021) 19–37, https://doi.org/10.1007/978-3-030-51652-9_2/FIGURES/5.

[15] S. Alves, A. Paris, E. Rathahao-Paris, Mass spectrometry-based metabolomics for an in-depth questioning of human health, Adv. Clin. Chem. 99 (2020) 147–191, https://doi.org/10.1016/BS.ACC.2020.02.009.

[16] S.C. Bendall, G.P. Nolan, M. Roederer, P.K. Chattopadhyay, A deep profiler's guide to cytometry, Trends Immunol. 33 (2012) 323–332, https://doi.org/10.1016/J.IT.2012.02.010.

[17] D. Pieragostino, S. Bucci, L. Agnifili, V. Fasanella, S. D'Aguanno, A. Mastropasqua, M. Ciancaglini, L. Mastropasqua, C. Di Ilio, P. Sacchetta, A. Urbani, P. Del Boccio, Differential protein expression in tears of patients with primary open angle and pseudoexfoliative glaucoma, Mol. Biosyst. 8 (2012) 1017–1028, https://doi.org/10.1039/C1MB05357D.

[18] A. Izzotti, M. Longobardi, C. Cartiglia, S.C. Saccà, Proteome alterations in primary open angle glaucoma aqueous humor, J. Proteome Res. 9 (2010) 4831–4838, https://doi.org/10.1021/PR1005372/SUPPL_FILE/PR1005372_SI_001.PDF.

[19] G. Tezel, Multiplex protein analysis for the study of glaucoma, Expert Rev. Proteomics 18 (2021) 911–924, https://doi.org/10.1080/14789450.2021.1996232.

[20] M.D. Pinazo-Durán, C. Galbis-Estrada, S. Pons-Vázquez, J. Cantú-Dibildox, C. Marco-Ramírez, J. Benítez-del-Castillo, Effects of a nutraceutical formulation based on the combination of antioxidants and ω-3 essential fatty acids in the expression of inflammation and immune response mediators in tears from patients with dry eye disorders, Clin. Interv. Aging 8 (2013) 139–148, https://doi.org/10.2147/CIA.S40640.

[21] C. Galbis-Estrada, M.D. Pinazo-Durán, J. Cantú-Dibildox, C. Marco-Ramírez, M. Díaz-Llópis, J. Benítez-del-Castillo, Patients undergoing long-term treatment with antihypertensive eye drops responded positively with respect to their ocular surface disorder to oral supplementation with antioxidants and essential fatty acids, Clin. Interv. Aging 8 (2013) 711–719, https://doi.org/10.2147/CIA.S43191.

[22] C. Galbis-Estrada, S. Martinez-Castillo, J.M. Morales, B. Vivar-Llopis, D. Monleón, M. Díaz-Llopis, M.D. Pinazo-Durán, Differential effects of dry eye disorders on metabolomic profile by 1H nuclear magnetic resonance spectroscopy, BioMed Res. Int. 2014 (2014), https://doi.org/10.1155/2014/542549.

[23] J. Benitez-del-Castillo, J. Cantu-Dibildox, S.M. Sanz-González, V. Zanón-Moreno, M.D. Pinazo-Duran, Cytokine expression in tears of patients with glaucoma or dry eye disease: a prospective, observational cohort study, Eur. J. Ophthalmol. 29 (2018) 437–443, https://doi.org/10.1177/1120672118795399.

[24] J.M. Benítez Del Castillo, M.D. Pinazo-Duran, S.M. Sanz-González, A.M. Muñoz-Hernández, J.J. Garcia-Medina, V. Zanón-Moreno, Tear 1H nuclear magnetic resonance-based metabolomics application to the molecular diagnosis of aqueous tear deficiency and meibomian gland dysfunction, Ophthalmic Res. 64 (2021) 297–309, https://doi.org/10.1159/000510211.

[25] S. Lereuz, A. Marill, T. Bresson, D. Saint Martin, C. Verny, P. Gohier, J. Muller, L. Tessier, P. Amati-bonneau, G. Lenaers, D. Bonneau, G. Simard, D. Milea, V. Procaccio, P. Reynier, J. Manuel, C. De, A metabolomics profiling of glaucoma points to mitochondrial dysfunction, senescence, and polyamines deficiency, Biochem. Mol. Biol. 59 (2018) 4355–4361, https://doi.org/10.1167/iovs.18-24938.

[26] Z. Zhang, L. Li, C. Zhang, P. Zhang, Z. Fang, J. Li, S. Wang, Relationship between plasma amino acid and carnitine levels and primary angle-closure glaucoma based on mass spectrometry metabolomics, Exp. Eye Res. 227 (2023), https://doi.org/10.1016/j.exer.2022.109366.

[27] S. Rong, Y. Li, Y. Guan, L. Zhu, Q. Zhou, M. Gao, H. Pan, L. Zou, D. Chang, Long-chain unsaturated fatty acids as possible important metabolites for primary angle-closure glaucoma based on targeted metabolomic analysis, Biomed, Chromatography 31 (2017) e3963, https://doi.org/10.1002/BMC.3963.

[28] E. Hodapp, R. Parrish, D.R. Anderson, Clinical decisions in glaucoma. https://api.semanticscholar.org/CorpusID:56639770, 1993. (Accessed 26 July 2023).

[29] O. Beckonert, H.C. Keun, T.M.D. Ebbels, J. Bundy, E. Holmes, J.C. Lindon, J. K. Nicholson, Metabolic profiling, metabolomic and metabonomic procedures for NMR spectroscopy of urine, plasma, serum and tissue extracts, Nat. Protoc. 2 (11) (2007) 2692–2703, https://doi.org/10.1038/nprot.2007.376, 2 (2007).

[30] D.S. Wishart, D. Tzur, C. Knox, R. Eisner, A.C. Guo, N. Young, D. Cheng, K. Jewell, D. Arndt, S. Sawhney, C. Fung, L. Nikolai, M. Lewis, M.A. Coutouly, I. Forsythe, P. Tang, S. Shrivastava, K. Jeroncic, P. Stothard, G. Amegbey, D. Block, D.D. Hau, J. Wagner, J. Miniaci, M. Clements, M. Gebremedhin, N. Guo, Y. Zhang, G. E. Duggan, G.D. MacInnis, A.M. Weljie, R. Dowlatabadi, F. Bamforth, D. Clive, R. Greiner, L. Li, T. Marrie, B.D. Sykes, H.J. Vogel, L. Querengesser, HMDB: the human metabolome database, Nucleic Acids Res. 35 (2007) 521–526, https://doi.org/10.1093/nar/gkl923.

[31] J.C. Hoch, K. Baskaran, H. Burr, J. Chin, H.R. Eghbalnia, T. Fujiwara, M.R. Gryk, T. Iwata, C. Kojima, G. Kurisu, D. Maziuk, Y. Miyanoiri, J.R. Wedell, C. Wilburn, H. Yao, M. Yokochi, Biological magnetic resonance data bank, Nucleic Acids Res. 51 (2023) D368–D376, https://doi.org/10.1093/nar/gkac1050.

[32] J. Chong, O. Soufan, C. Li, I. Caraus, S. Li, G. Bourque, D.S. Wishart, J. Xia, MetaboAnalyst 4.0: towards more transparent and integrative metabolomics analysis, Nucleic Acids Res. 46 (2018) W486–W494, https://doi.org/10.1093/NAR/GKY310.

[33] R.N. Weinreb, T. Aung, F.A. Medeiros, The pathophysiology and treatment of glaucoma: a review, JAMA 311 (2014) 1901–1911, https://doi.org/10.1001/JAMA.2014.3192.

[34] L. Agnifili, D. Pieragostino, A. Mastropasqua, V. Fasanella, L. Brescia, G.M. Tosi, P. Sacchetta, L. Mastropasqua, Molecular biomarkers in primary open-angle glaucoma: from noninvasive to invasive, Prog. Brain Res. 221 (2015) 1–32, https://doi.org/10.1016/BS.PBR.2015.05.006.

[35] J. Wu, M. Xu, W. Liu, Y. Huang, R. Wang, W. Chen, L. Feng, N. Liu, X. Sun, M. Zhou, K. Qian, Glaucoma characterization by machine learning of tear metabolic fingerprinting, Small Methods 6 (2022) 1–10, https://doi.org/10.1002/smtd.202200264.

[36] C. Myer, J. Perez, L. Abdelrahman, R. Mendez, R.B. Khattri, A.K. Junk, S. K. Bhattacharya, Differentiation of soluble aqueous humor metabolites in primary open angle glaucoma and controls, Exp. Eye Res. 194 (2020) 108024, https://doi.org/10.1016/j.exer.2020.108024.

[37] A. Buisset, P. Gohier, S. Leruez, J. Muller, P. Amati-Bonneau, G. Lenaers, D. Bonneau, G. Simard, V. Procaccio, C. Annweiler, D. Milea, P. Reynier, J.M. Chao De La Barca, Metabolomic profiling of aqueous humor in glaucoma points to taurine and spermine deficiency: findings from the eye-D study, J. Proteome Res. 18 (2019) 1307–1315, https://doi.org/10.1021/acs.jproteome.8b00915.

[38] X. Chen, Y. Chen, L. Wang, X. Sun, Metabolomics of the aqueous humor in patients with primary congenital glaucoma, Mol. Vis. 25 (2019) 489–501.

[39] J.M. Tiffany, The normal tear film, in: G. Geerling, H. Brewitt (Eds.), Surg. Dry Eye Sci. Evid. Guidel. Clin. Manag. Dry Eye Assoc. Ocul. Surf. Dis., S.Karger AG, 2008, https://doi.org/10.1159/000131066, p. 0.

[40] R. Mastropasqua, V. Fasanella, E. Pedrotti, M. Lanzini, S. Di Staso, L. Mastropasqua, L. Agnifili, Trans-conjunctival aqueous humor outflow in glaucomatous patients treated with prostaglandin analogues: an in vivo confocal microscopy study, Graefe's Arch. Clin. Exp. Ophthalmol. 252 (2014) 1469–1476, https://doi.org/10.1007/s00417-014-2664-9.

[41] C. Rossi, I. Cicalini, M.C. Cufaro, L. Agnifili, L. Mastropasqua, P. Lanuti, M. Marchisio, V. De Laurenzi, P. Del Boccio, D. Pieragostino, Multi-omics approach for studying tears in treatment-naïve glaucoma patients, Int. J. Mol. Sci. 20 (2019) 1–14, https://doi.org/10.3390/ijms20164029.

[42] J. Barbosa-Breda, U. Himmelreich, B. Ghesquière, A. Rocha-Sousa, I. Stalmans, Clinical metabolomics and glaucoma, Ophthalmic Res. 59 (2017) 1–6, https://doi.org/10.1159/000479158.

[43] Y. Wang, X.W. Hou, G. Liang, C.W. Pan, Metabolomics in glaucoma: a systematic review, Investig. Ophthalmol. Vis. Sci. 62 (2021) 1–8, https://doi.org/10.1167/IOVS.62.6.9.

[44] A. Umeno, M. Tanito, S. Kaidzu, Y. Takai, M. Horie, Y. Yoshida, Comprehensive measurements of hydroxylinoleate and hydroxyarachidonate isomers in blood samples from primary open-angle glaucoma patients and controls, Sci. Rep. 9 (2019) 1–11, https://doi.org/10.1038/s41598-018-36952-6.

[45] S. Javadiyan, K.P. Burdon, M.J. Whiting, S. Abhary, T. Straga, A.W. Hewitt, R. A. Mills, J.E. Craig, Elevation of serum asymmetrical and symmetrical dimethylarginine in patients with advanced glaucoma, Invest. Ophthalmol. Vis. Sci. 53 (2012) 1923–1927, https://doi.org/10.1167/iovs.11-8420.

[46] O.A. Zeleznik, J.H. Kang, J. Lasky-Su, A.H. Eliassen, L. Frueh, C.B. Clish, B. A. Rosner, T. Elze, P. Hysi, A. Khawaja, J.L. Wiggs, L.R. Pasquale, Plasma metabolite profile for primary open-angle glaucoma in three US cohorts and the UK Biobank, Nat. Commun. 14 (2023) 2860, https://doi.org/10.1038/s41467-023-38466-w.

[47] J. Barbosa Breda, A. Croitor Sava, U. Himmelreich, A. Somers, C. Matthys, A. Rocha Sousa, E. Vandewalle, I. Stalmans, Metabolomic profiling of aqueous humor from glaucoma patients - the metabolomics in surgical ophthalmological patients (MISO) study, Exp. Eye Res. 201 (2020) 108268, https://doi.org/10.1016/j.exer.2020.108268.

[48] J.N.C. Bailey, B.L. Yaspan, L.R. Pasquale, M.A. Hauser, J.H. Kang, S.J. Loomis, M. Brilliant, D.L. Budenz, W.G. Christen, J. Fingert, D. Gaasterland, T. Gaasterland, P. Kraft, R.K. Lee, P.R. Lichter, Y. Liu, C.A. McCarty, S.E. Moroi, J.E. Richards, T. Realini, J.S. Schuman, W.K. Scott, K. Singh, A.J. Sit, D. Vollrath, G. Wollstein, D. J. Zack, K. Zhang, M.A. Pericak-Vance, R.R. Allingham, R.N. Weinreb, J.L. Haines, J.L. Wiggs, Hypothesis-independent pathway analysis implicates GABA and Acetyl-CoA metabolism in primary open-angle glaucoma and normal-pressure glaucoma, Hum. Genet. 133 (2014) 1319–1330, https://doi.org/10.1007/s00439-014-1468-7.

[49] H. Murai, Y. Suzuki, M. Kiyosawa, A.M. Tokumaru, K. Ishiwata, K. Ishii, Cerebral glucose metabolism in the striate cortex positively correlates with fractional anisotropy values of the optic radiation in patients with glaucoma, Clin. Exp. Ophthalmol. 43 (2015) 711–719, https://doi.org/10.1111/ceo.12543.

[50] C. Qian, S. Nusinovici, S. Thakur, Z. Da Soh, S. Majithia, M.L. Chee, H. Zhong, Y. C. Tham, C. Sabanayagam, P.G. Hysi, C.Y. Cheng, Machine learning identifying peripheral circulating metabolites associated with intraocular pressure alterations, Br. J. Ophthalmol. (2022) 1–6, https://doi.org/10.1136/bjophthalmol-2021-320584.

[51] T. Boillot, S.G. Rosolen, T. Dulaurent, F. Goulle, P. Thomas, P.F. Isard, T. Azoulay, S. Lafarge-Beurlet, M. Woods, S. Lavillegrand, I. Ivkovic, N. Neveux, J.A. Sahel, S. Picaud, N. Froger, Determination of morphological, biometric and biochemical susceptibilities in healthy eurasier dogs with suspected inherited glaucoma, PLoS One 9 (2014) e111873, https://doi.org/10.1371/journal.pone.0111873.

[52] A. Mayordomo-Febrer, M. López-Murcia, J.M. Morales-Tatay, D. Monleón-Salvadó, M.D. Pinazo-Durán, Metabolomics of the aqueous humor in the rat glaucoma model induced b-y a series of intracamerular sodium hyaluronate injection, Exp. Eye Res. 131 (2015) 84–92, https://doi.org/10.1016/j.exer.2014.11.012.